**Original Research Article**

Spectroscopic, Molecular Docking and Semi-Empirical Studies of the Albumin Binding Activities of 5-Hydroxymethylfurfural and its Synthesized Derivative, Di (5-Furfural) Ether

Olusegun Emmanuel Thomas*, Rashidat Temitope Oduwole

Department of Pharmaceutical Chemistry, Faculty of Pharmacy, University of Ibadan, Ibadan 200284, Nigeria

ARTICLE INFO**Article history**

Submitted: 2022-07-01

Revised: 2022-07-30

Accepted: 2022-09-25

Available online: 2022-09-29

Manuscript ID: PCBR-2207-1226

DOI: 10.22034/pcbr.2022.349903.1226

KEYWORDS

Hydroxymethylfurfural

5,5'-oxydimethylenebis(2-furfural)

Synthesis

Spectroscopic characterization

Quantum

Mechanical calculations

ABSTRACT

Previous studies have investigated the safety of the food/drug additive, 5-hydroxymethylfurfural including its albumin binding which might impact on its biodistribution and toxicity. In contrast, the safety assessment of its major degradant, di (5-furfural) ether (OMBF) is often neglected despite having been detected at concentrations in excess of HMF in parenteral solutions. The aim of this study was to compare the albumin binding characteristics of OMBF with 5-hydroxymethylfurfural. OMBF was synthesized by thermal dehydration of 5-hydroxymethylfurfural and characterized by using spectroscopic and mass spectral techniques. The binding characteristics of 5-hydroxymethylfurfural and OMBF with bovine serum albumin (BSA) were elucidated by using UV-visible spectroscopy, molecular docking, and semi-empirical calculations.

Photometric titrations with OMBF revealed more pronounced perturbations in the UV-visible spectra of BSA and binding constants that were 51% greater than those of 5-hydroxymethylfurfural. Thermodynamic parameters revealed that the OMBF binding to albumin was spontaneous and hydrophobic interactions were the main forces responsible for complex stabilization. Docking studies showed that the superior binding affinity of OMBF was due to its higher C/H ratio which facilitated an extensive network of six hydrophobic interactions with Tyr149, Leu237, Ala290, Ile289, and Arg194 residues of BSA Site I compared with only two hydrophobic interactions in 5-hydroxymethylfurfural complex. Analysis of the multi-point hydrogen bonded complexes by using PM6-D3H+ method revealed the interaction energy of OMBF-BSA complex was 1.5 folds greater than 5-hydroxymethylfurfural-BSA.

The study confirmed an increased avidity and stability in the complexation of albumin with OMBF compared with 5-hydroxymethylfurfural. Stricter limits control of OMBF in heat-processed foods/drugs is necessary.

* Corresponding author: Olusegun Emmanuel Thomas

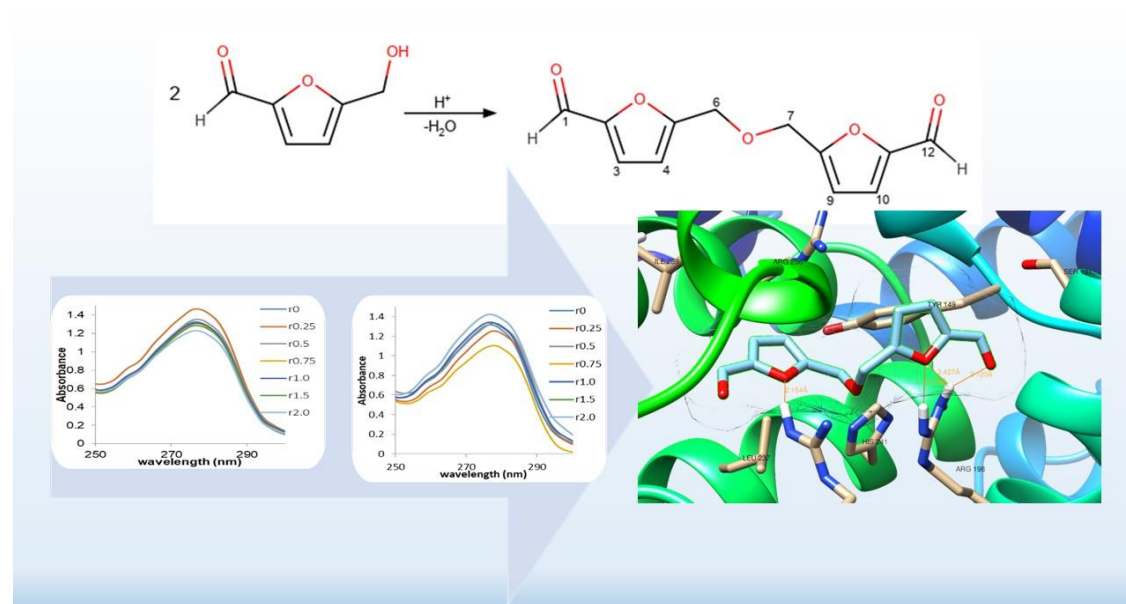
✉ E-mail: seguntom@yahoo.com

☎ Tel number: +2348034198737

© 2022 by SPC (Sami Publishing Company)



GRAPHICAL ABSTRACT



1-Introduction

The compound, 5-hydroxymethylfurfural (HMF), is a product of Maillard reaction that is generated during the heat processing of sugar-containing foods and parenteral solutions [1]. HMF is found at the average levels that vary widely from 1.4 mg/kg in whiskey to 2000 mg/kg in instant coffee and over 9000 mg/kg in caramel products [1, 2]. HMF is also present in heat-sterilised parenteral solutions and traditional Chinese medicines [3]. The HMF formation is directly related to the applied heat load and although not often present in fresh foods, HMF rapidly accumulates during heat treatment [1]. Thus, HMF content is often used as an indicator of food quality and over-processing of foods [4]. HMF has also been employed in the food industry as an additive to impart characteristic flavour and encourage customer acceptability [1]. The possibility of intolerably high levels of HMF in products as a result of over-processing and/or its deliberate inclusion as an additive raises potential safety concerns. While its protective effect against oxidative stress and hypoxia are well reported, a few studies have also indicated a link between HMF exposure from drug

formulations and clinical presentations such as allergies, muscle damage, and thrombophlebitis [3, 5]. In addition, HMF showed contradicting results with different genotoxicity assay models: some studies have documented that the compound is not mutagenic with or without activation in the Salmonella mutation test, other reports have established an enzymatic conversion into an active metabolite, 5-sulfoxymethylfurfural with mutagenicity towards *S. typhimurium* TA104 [6–8]. Significant DNA damage when measured by end-point parameters such as single-strand breaks, micronuclei frequency, chromosomal aberrations, and sister-chromatid exchange have been further reported with HMF [8–10]. Likewise, a previous study had documented an extensive *in vitro* binding of HMF with albumin *via* hydrogen bonding and hydrophobic interactions [11]. The *in vitro* investigation of the binding dynamics between molecules and the major transporter protein, albumin which has two major binding sites known as Sites I and II, remains central in the safety assessment of chemical compounds as it dictates their distribution, access to storage sites, and toxicity [12]. This is particularly critical

for additives for which bioaccumulation following consumption of sub-toxic levels over time has been identified as a major contributor to their toxicity [13]. However, while HMF has been the subject of several studies investigating its toxicity liabilities, the well-known ability of the compound to undergo degradative reactions and react with several other food components has not resulted in a similar extensive investigation of its degradative/reaction products. Amongst several other degradative routes, HMF can be decarboxylated to furfural, oxidised to 2,5-furandialdehyde or 5-hydroxymethyl-2-furan carboxylic acid, reduced to 5-methylfufural or undergo dimeric condensation to yield di (5-furfural) ether otherwise called 5,5'-oxydimethylenebis (2-furfural) (OMBF) [14]. We have taken particular interest in the safety profile of OMBF (Figure 1b) as it is readily generated from the self-condensation of HMF and at elevated temperatures similar to those required for the initial formation of HMF in foods. Furthermore, it has been established that the HMF concentration formed during Maillard reaction exists in equilibrium with the OMBF concentration [1,15]. Moreover, HMF readily

degrades to OMBF during prolonged storage of foods and medicines. Thus, OMBF has been found in stored parenteral solutions at concentrations greater than those of HMF [3]. It is certain that the relative levels of OMBF in products might pose safety concerns which are equal if not greater than those of HMF as revealed by a recent study that reported the higher immune sensitisation potential of OMBF [3]. Unfortunately, there continues to be a dearth of investigations on the potential toxicity of OMBF to human health. In this study, we focus on the albumin binding dynamics of the compounds and hypothesised that the higher aromatic character of OMBF might substantially alter its albumin binding compared with HMF. To the best of our knowledge, this study represents the first *in vitro* investigation of the binding dynamics of OMBF with endogenous macromolecules.

The objective of this study was therefore to delineate the binding affinities and intermolecular forces of interactions involved in the formation of albumin-HMF and albumin-OMBF complexes by using spectroscopic, molecular docking, and semi-empirical methods.

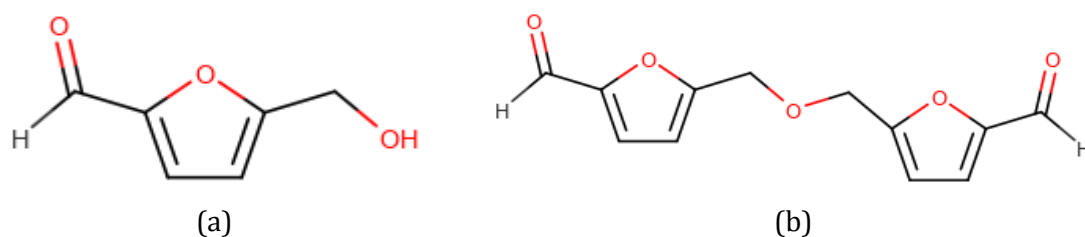


Fig. 1. Chemical structures of (a) 5-hydroxymethylfurfural and (b) 5,5'-oxydimethylenebis (2-furfural)

2- Experimental

2-1-Materials

5-hydroxymethylfurfural (AK Scientific), Bovine serum albumin (Glentham UK), Tris base (Sigma Aldrich), and Hydrochloric acid (BDH UK).

2-2- Equipment

UV-visible spectrophotometer with 1 cm path length (Spectroquant Pharo 300), NMR 60 MHz

(Nanalysis 60PRO Multinuclear), IR spectrophotometer (Buck Scientific M530), HPLC (Agilent Technologies 1290 Infinity), and Mass spectrometer (Agilent Infinity G6125B).

2-3-Sample preparation

Tris-HCl buffer solution of pH=7.4 was prepared by careful addition of concentrated hydrochloric acid to 10 mM Tris base solution. A 3×10^{-5} M

stock solution of BSA in Tris-HCl buffer, 1.8×10^{-3} M stock solution of HMF in Tris-HCl buffer and 1.8×10^{-3} M stock solution of OMBF in 10% aqueous DMSO were prepared. Thereafter working concentrations of the ligands equivalent to 45, 90, 135, 180, 270, and 360 μ M in Tris-HCl buffer were prepared.

2-4- Synthesis and characterization of OMBF

OMBF was synthesized by the thermal dehydration of 5-hydroxymethylfurfural [16]. A 0.29 mL aliquot of DMSO (that has been previously dried over activated alumina for 24 hours) was added to 5.45 g of HMF in a round bottomed flask. The mixture was refluxed at 155 °C for one hour after which it was cooled in an ice-bath before the addition of 50 mL water. The mixture was refluxed for an additional 30 minutes, filtered, and cooled to obtain needle-like crystals which were collected by filtration and dried in a desiccator. The IR, mass spectral data, the ^1H , and ^{13}C NMR characterization of the synthesized compound with respect to the residual proton of DMSO- d_6 were obtained at room temperature.

2-5- Binding experiments

Aliquots of the ligand solutions were added to a fixed concentration of BSA to obtain $r_i = [\text{ligand}]/[\text{BSA}]$ values of 0, 0.25, 0.5, 0.75, 1.0, 1.5, and 2.0. The final volume of all the reaction mixtures was made up to 5 mL with Tris-HCl buffer solution, and then allowed to equilibrate for 30 minutes at 25 °C. After that, the UV-visible spectra of BSA in the absence and presence of the ligands were acquired from 190 to 420 nm by using the corresponding ligand solution for baseline correction of the spectrophotometer. The entire procedure was repeated at 37 °C.

The binding constants of the ligands were determined at the two temperature levels from Benesi-Hilderbrand plots by using Equation (1).

$$\frac{A^*}{A-A^*} = \frac{\varepsilon G}{\varepsilon H - G - \varepsilon G} + \frac{\varepsilon G}{\varepsilon H - G - \varepsilon G} \frac{1}{K_f[\text{ligand}]} \quad (1)$$

Where, A^* and A refer to the absorbances of BSA in the absence and presence of ligand, respectively and, εG and $\varepsilon H - G$ are their molar absorptivities. The thermodynamic enthalpy (ΔH) and entropy (ΔS) energy changes associated with ligand-protein complex formation were determined from a modified Van't Hoff plot (2) and (3), respectively.

$$\ln \frac{k_2}{k_1} = -\frac{\Delta H^\circ}{R} \left(\frac{1}{T_2} - \frac{1}{T_1} \right) \quad (2)$$

$$\Delta G = \Delta H - T\Delta S \quad (3)$$

2-6- Molecular docking

The Open Babel plugin in PyRx was used to minimize and convert the 3D structures of the ligands into the dockable format. The crystallographic structure of bovine serum albumin (PDB ID: 3V03) was downloaded from the RCSB protein data bank (PDB) and prepared by using Chimera 1.16 software. The chain B monomer of the protein, complexed ions, and non-standard amino acid residues were deleted before minimizing. Solvent molecules were then removed followed by the addition of hydrogen and charges by using the Gastelger force field. The multiple docking of the ligands and proteins were carried out by using the virtual screening tool, PyRx incorporated with Autodock Vina 1.1.2 software [17]. An initial blind docking with grid box size of 94.44x79.74x101.24 centered at $x = 97.64$, $y = 27.72$, $z = 23.49$ Å identified the preferential binding of the ligands to Site I of BSA. Thereafter, Site I-directed docking by using grid box size of 31.46x19.19x40.71 and centered at $x = 29.58$, $y = 32.97$, $z = 31.80$ Å was carried out. Post docking analysis of the conformations, type, and strength of intermolecular forces involved in ligand-protein complexation were done by using UCSF Chimera 1.16 and Biovia Discovery Studio Visualiser 2020 software.

2-7- Semi-empirical quantum mechanical calculations

The geometrical parameters of the protein-ligand complexes were optimized by using PM6-D3H+

which is a third-generation hydrogen bonding-corrected semi-empirical method [18]. Likewise, vibrational frequencies of the complexes were evaluated with the same method. By using the supermolecular approach with counterpoise correction, interaction energy of the complexes were determined as:

$$\Delta E^{int} = E(AB) - E(A) - E(B) \quad (4)$$

Where, E(AB), E(A), and E(B) refer to the electronic energies of the complex and its constituents, A and B, respectively. All calculations were done by using the GAMESS programme [19].

3- Results and Discussion

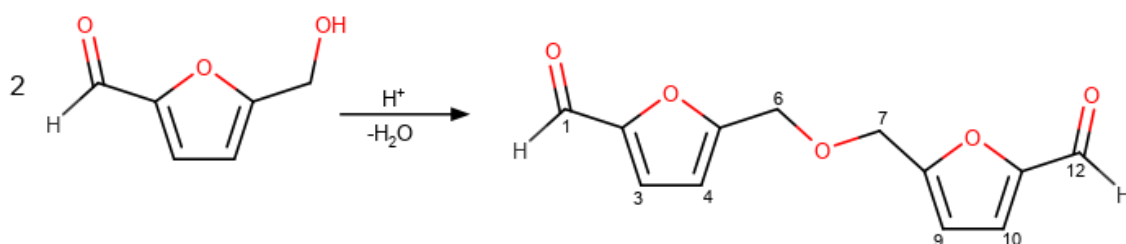
3-1- Spectral data of OMBF

Colour: yellow; mp: 111-113 °C; Yield: 27.5%; IR (KBr) cm^{-1} : 2690.47-2782.47 (aldehyde H), 1600.0 (C=O), 1289.60 (C-O); ^1H NMR (DMSO- d_6

60MHz) δ : 9.54 (s, 2H CHO), 7.45 (d, $J= 3.6$ Hz, 2H), 6.70 (d, $J= 3.6$ Hz, 2H), 4.58 (s, 4H); ^{13}C NMR (DMSO- d_6 60MHz) δ : 178.78 (C-1 and C-12), 157.72 (C-5 and C-8), 152.81 (C-2 and C-11), 123.99 (C-3 and C-10), 112.66 (C-4 and C-9), 64.19 (C-6 and C-7); negative-ion ESI: m/z molecular ion peak not found, calculated M 234.2

3-2- Synthesis and structural elucidation of OMBF

Thermal dehydration of HMF in the presence of dry DMSO yielded yellow needle-shaped crystals of OMBF with a yield of 27.5%. The purity of the product as determined by liquid chromatography was 95.72%w/w. The overall reaction scheme is depicted in Scheme 1. Dry DMSO can catalyse ether formation from alcohols in a self-condensation reaction which proceeds *via* a resonance-stabilised carbocation [16].



Scheme 1. Synthesis of 5, 5'-oxydimethylenebis (2-furfural) *via* thermal dehydration of 5-hydroxymethylfurfural

This reaction, which has been successfully used for the synthesis of benzylic and allylic ethers from benzyl and allylic alcohols, respectively, yielded OMBF in sufficiently high purity of 95.72%w/w [20, 21]. The chemical shifts, reported with respect to the residual protons of the deuterated solvent, were consistent with predicted values. The chemical shift values were readily assigned by using the de-shielding effects and splitting patterns of the peaks. Expectedly, the mass spectrum of OMBF did not produce a molecular ion because ethers are very unstable to ionisation energy in mass spectrometry [22]. Characteristically as with ethers, the oxygen atom mediated the fragmentation of OMBF

leading to a β -cleavage that is stabilised by resonance [23]. Thus, the mass spectrum of OMBF (as demonstrated in supplemental files) revealed a base peak of m/z value of 108.6 corresponding to the $\text{C}_5\text{H}_3\text{O}_2\text{-CH}_2^+$ fragment. Another peak of m/z value of 138.6, but with lower relative abundance could also be observed and this was attributed to $\text{C}_6\text{H}_5\text{O}_3\text{-CH}_2^+$ fragment.

3-3- Spectroscopic characterization of BSA binding

Incremental addition of 5-hydroxymethylfurfural to a fixed concentration of BSA produced an initial increase in the absorption of its 278 nm band which was then followed by a progressive decrease in the absorption intensity, as displayed

in Figure 2. On the other hand, with OMBF titration, an initial decrease in the 278 nm band

was observed before a progressive increase in absorption intensity.

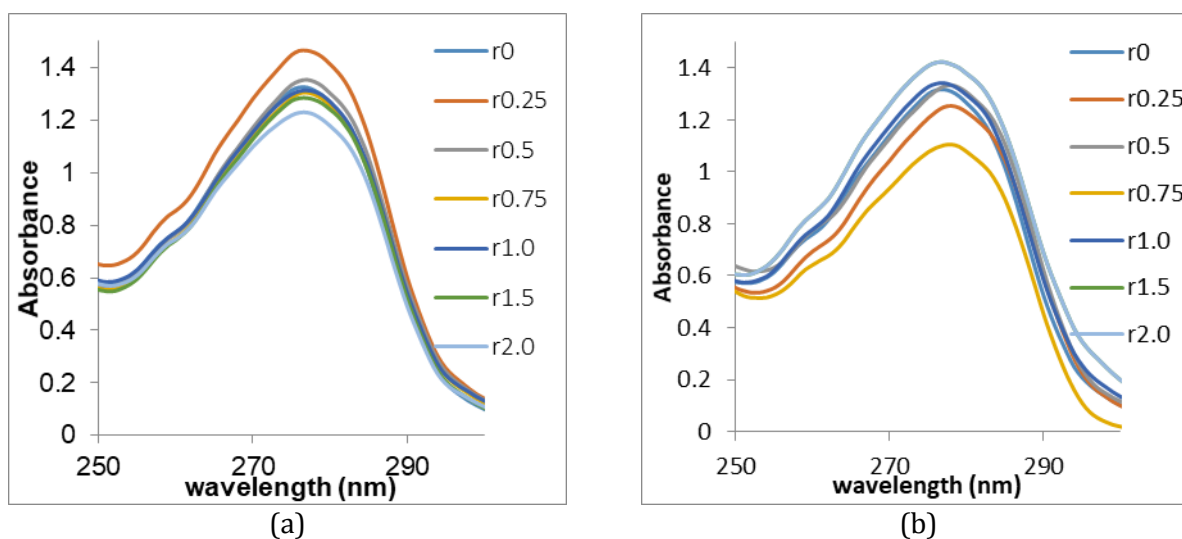


Fig. 2. Changes in the UV absorption spectra of BSA with titration of (a) HMF and (b) OMBF

The Benesi-Hilderbrand plots for the binding of the ligands with albumin at 25 °C and 37°C are depicted in Figure 3. The plots showed a linear relationship ($R^2 > 0.9$) between $A_0/A - A_0$ and reciprocal of ligand concentration in the protein

complex. The slope of the double reciprocal plots at both temperatures investigated further revealed that OMBF produced more pronounced changes in the response parameter for the same concentrations of HMF.

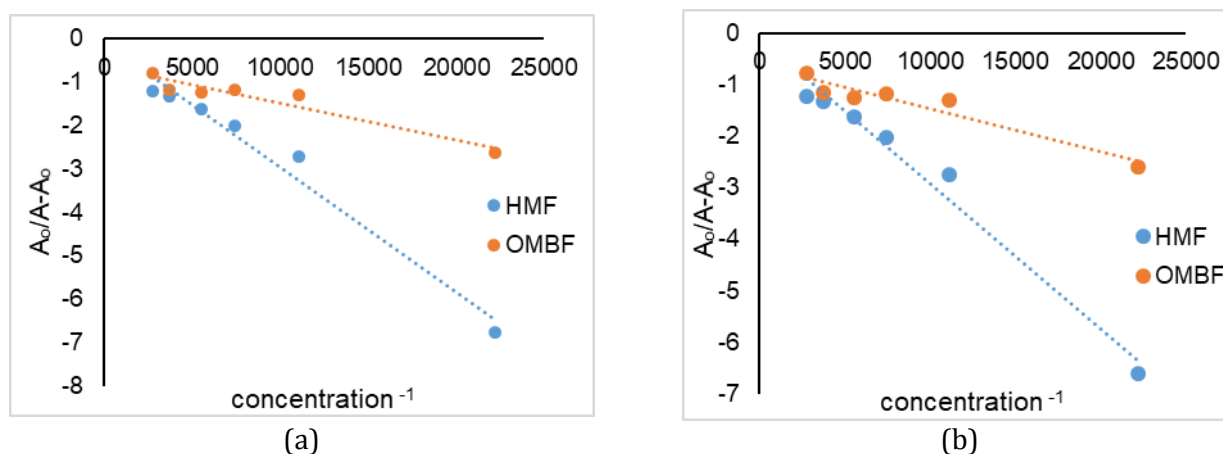


Fig. 3. Benesi-Hilderbrand plots for the formation of ligand-BSA complex at (a) 25 °C and (b) 37 °C

The binding or formation constants were estimated from the ratio of the intercept to the slope of the plots and are listed in Table 1. The thermodynamic changes, free energy (ΔG),

enthalpy (ΔH), and entropy (ΔS) associated with ligand-protein complex formation are also represented in Table 1.

Table 1. Binding and thermodynamic energy changes associated with interaction of albumin with ligands

Interactions	25 °C		37 °C		ΔH (KJ/mol)	ΔS (KJ/mol)
	$\ln K_f$	ΔG (KJ/mol)	$\ln K_f$	ΔG (KJ/mol)		
5 HMF-BSA	5.35	-13.26	5.97	-14.78	39.43	0.18
OMBF-BSA	8.98	-22.26	8.99	-22.29	0.83	0.08

The UV-visible spectroscopy can be used to study protein-ligand complexation and the effects of the interaction on the structural conformation of proteins. Bovine serum albumin indicated two characteristic bands at 220 and 278 nm. The high intensity band at 220 nm was attributed to the $\pi - \pi^*$ transition of C=O functional groups in the BSA peptide backbone, while the 278 nm band is ascribed to the $\pi - \pi^*$ transition of its aromatic amino acid residues including tryptophan, tyrosine, and phenylalanine [24,25]. The observed changes in the 278 nm band of BSA following titration with HMF or OMBF arose from the hydrophobic interactions between the aromatic rings of these amino acids and the ligands. These changes are indicative of perturbations in the BSA conformation which might include an unfolding of the backbone and a reduction of its hydrophobicity [26].

The formation constants of both HMF-albumin and OMBF-albumin complexes increased with temperature indicating an endothermic process [24]. Binding affinity is a function of structural chemistry and as a result, derivatives of a ligand (metabolite, degradation products, etc.) might show different binding profiles and affinities compared with the intact ligand. The formation constant of a ligand-BSA complex is a measure of binding affinity, thus a higher binding constant indicates an increased affinity of the ligand for the protein. The binding affinity of a ligand influences both its pharmacokinetic and pharmacodynamics properties including its therapeutic effectiveness, *in vivo* stability, and toxicity [27]. Increased binding to albumin might prolong the storage time of a ligand in the body leading to bioaccumulation which has been

previously identified as a major cause of toxicity of food additives and contaminants [13, 28]. Thus, compared with HMF, the dimer OMBF which showed more than 51% increased affinity for albumin at both investigated temperatures might be more prone to bioaccumulation and toxicity. In a previous comparison of its immunomodulatory capability with HMF, OMBF showed substantial immune sensitisation potential which may contribute to the autoimmune diseases often reported with traditional Chinese Medicine injections [3]. Increased affinity further indicated that OMBF might be better transported by circulating albumin which often serves as an *in vivo* solubilizing agent increasing the access of otherwise insoluble ligands to the storage tissues [29].

3-4-Thermodynamic parameters and intermolecular forces of interaction

Ligand-protein complexation is often driven by reversible forces of interaction including hydrogen bonding, hydrophobic forces, Van der Waals, and electrostatic interactions. The thermodynamic parameters associated with a complex formation between albumin and the ligands were therefore calculated to determine the prominent forces responsible for complex stabilization (Table 1). The negative value of ΔG showed that all the binding processes were spontaneous. According to the previous studies on ligand-protein interactions, a combination of positive enthalpic and entropic changes are indicative of predominating hydrophobic forces [30, 31]. Thus, the formation and stabilization of HMF-BSA and OMBF-BSA complexes were driven by hydrophobic forces presumably between the aromatic furan rings of the ligands and the

hydrophobic pocket of albumin. Expectedly, compared with HMF, the more extensive aromatic structure of OMBF increased its hydrophobic interactions and binding affinity with BSA. These results are in agreement with an earlier fluorescence spectroscopic study identified hydrophobic forces as responsible for the HMF binding with human serum albumin [11].

3-5- Molecular docking characterization of thermodynamics of BSA binding

Molecular modelling revealed that HMF and OMBF bound to BSA site I with binding energies of -5.3 kcal/mol RMSD = 0 and -7.2 kcal/mol, RMSD = 0, respectively. Both ligands occupied the hydrophobic pocket of site I in albumin, as illustrated in Figure 4. The schematic representation of the interaction of amino acid residues in the subdomain IIA of albumin with HMF and OMBF are displayed in Figures 5 and 6, respectively.

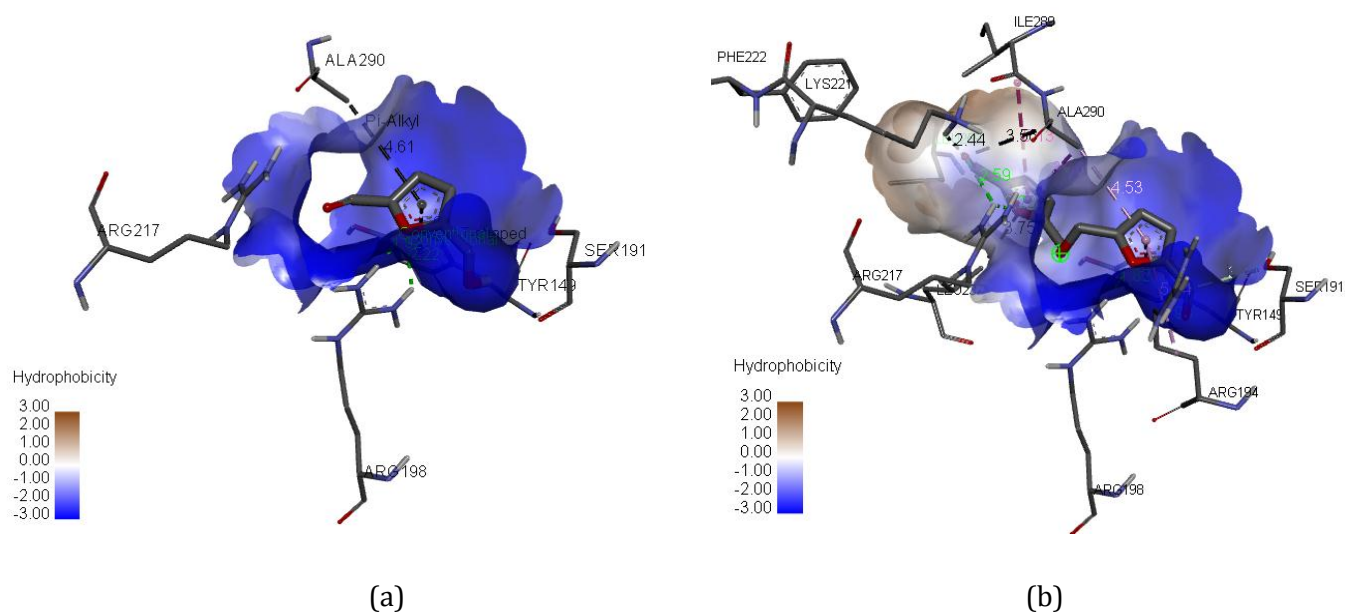


Fig. 4. Orientations of (a) HMF and (b) OMBF within the hydrophobic pocket of BSA site-I

Molecular docking is one of several approaches in computer-aided drug design to understand protein-ligand interaction and stabilization. When employed prior to the experimental bioassay in drug discovery, molecular docking serves as a powerful computational filter that can save resources [25]. On the other hand, when deployed to validate experimental results, docking studies provide a useful insight to the mechanisms of ligand-protein interactions and how these can be modified to improve pharmacokinetics of lead compounds including

distribution, drug-drug interactions, metabolic liabilities, promiscuity, etc.

There are three binding sites in albumin with majority of bound drugs occupying either Site I which is the subunit domain IIA of BSA containing tryptophan 213 residue or Site II (the subunit domain IIIA of BSA) that include tryptophan 134 residue [25, 32]. In this study, blind docking showed that HMF and OMBF preferentially bound at Site I which was identified by warfarin, a Site I marker.

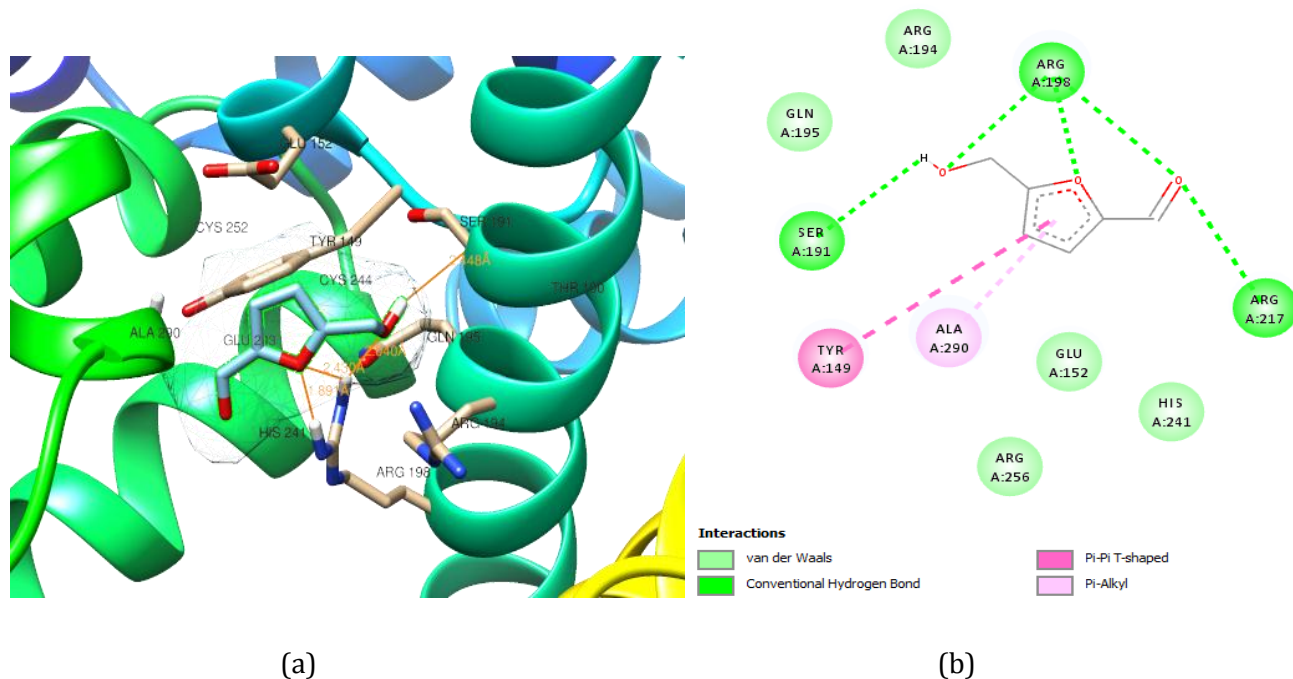


Fig. 5. (a) 3D view and (b) 2D representation of molecular interaction of HMF with BSA site-I

Site-directed docking revealed that HMF and OMBF were inserted into the hydrophobic pockets of subunit domain IIA of albumin and were surrounded by amino acids which vary in hydrophobicity, polarity, and charge. However, HMF and OMBF showed a graded affinity for albumin with binding energies of -5.3 and -7.2 kcal/mol, respectively when compared with -8.2 kcal/mol obtained by warfarin. Although this represents to the best of our knowledge, the first docking study with OMBF, our modelling protocol was further validated as it corroborated previous fluorescence spectroscopic and docking studies which identified subdomain IIA of human serum albumin as the binding site of HMF [11,33]. These previous studies further documented a similar array of surrounding amino acids residues in the binding pocket of HMF as we have herein reported. The marked difference in the affinities of HMF and OMBF for BSA, as reported in our study, can be attributed to the type and extent of their intermolecular interactions with albumin which is in turn dictated by their chemical structure. HMF interacted through five hydrogen bonds, four of which involved oxygen atoms in its heterocyclic ring and side chains. The

guanidinium ion of Arginine 198 was involved in two hydrogen bonds with oxygen of the furan ring (bond lengths of 1.89 and 2.43Å) and in a third hydrogen bond (predicted bond length of 2.04Å) with oxygen of alcohol side group of the ligand. Likewise, a fourth hydrogen bond (predicted bond length 3.02Å) between the ketonic group of HMF and Arginine 217 could be observed in the 2D representation. At physiological pH, the side chain of arginine can accept proton and become positively charged [34]. The positive charge is sufficiently stabilised by the resonance of its guanidinium ion and can drive the extensive interaction of the amino acid residue with the electronegative oxygen atoms of HMF. The fifth hydrogen bond interaction of HMF with a predicted bond length of 2.448Å involved its alcohol group serving as hydrogen bond donor and the side chain of Serine 191 as acceptor. Expectedly, OMBF which is a dimer of HMF showed a similar extensive network of hydrogen bond interactions with the guanidinium ions of Arginine 198, Arginine 217, and the side chain of Serine 191.

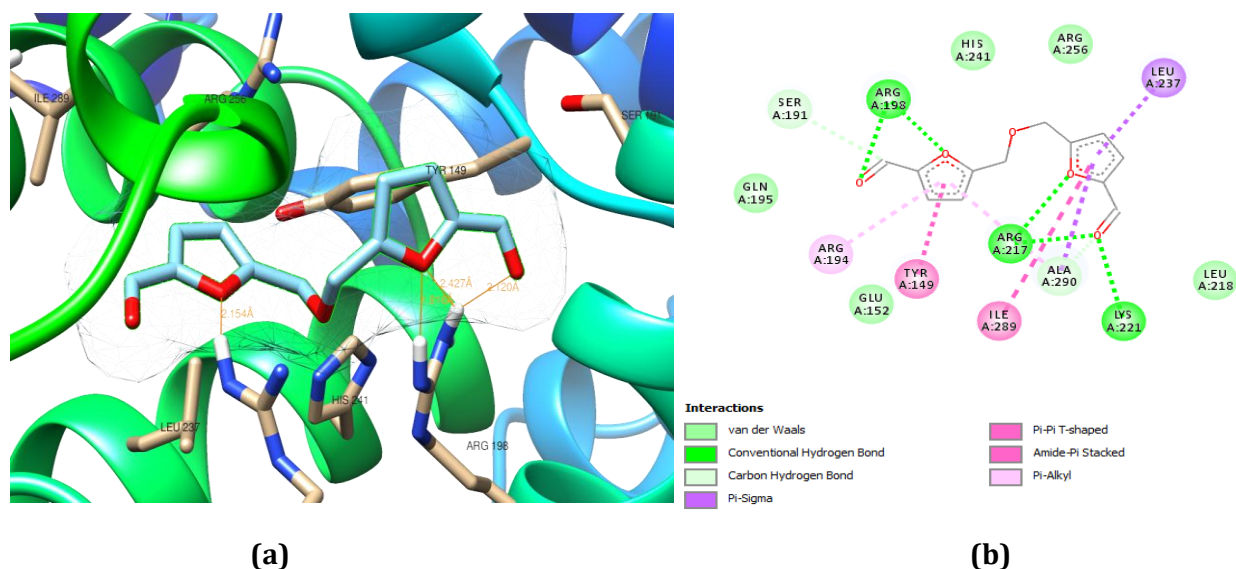


Fig. 6. (a) 3D view and (b) 2D representation of molecular interaction of OMBF with BSA site-I

In addition, a new hydrogen bond interaction involving the positively charged side chain of Lysine 221 and polar carbonyl group of OMBF could be observed. This additional intermolecular interaction may contribute to the increased binding of OMBF as obtained in docking studies. However, as previously identified in thermodynamic studies, hydrophobic interactions played prominent roles in driving the binding of both compounds and the stabilization of their resultant ligand-protein complexes. Thus, although docking indicated that both ligands occupied the hydrophobic pocket of site I of BSA and were surrounded by hydrophobic amino acid residues including Phe222, Ile289, Ala290, and Leu237, the marked difference in the albumin binding affinities of HMF and OMBF can be better explained by the predicted hydrophobic interactions, as displayed in Figures 5 and 6.

Analysis of the OMBF-albumin complex in Figure 6b showed six hydrophobic intermolecular forces in which the π -electrons of the furan rings of the ligand were involved in interactions with the saturated bond electrons of leucine 237 and alanine 290, aromatic π -electrons of tyrosine 149, amide functional groups of isoleucine 289, and the alkyl side chains of arginine 194 and

alanine 290, among which three interactions, on the account of their intermolecular distances, were regarded as significant. These included pi-sigma interactions with leucine 237 (3.75Å) and alanine 290 (3.56Å) as well as pi-alkyl interactions with alanine 290 (4.53Å). In contrast, as depicted in Figure 5b, only two hydrophobic interactions were involved in the stabilization of HMF-albumin complex *viz.* pi-pi T-shaped interaction with tyrosine 149 and pi-alkyl interaction with alanine 290. Of the two interactions, only the latter was significant with a bond length of 4.61Å. Hydrophobic interactions generally increase with number of carbon atoms in a molecule, and thus OMBF with a higher C/H ratio expectedly showed an increased propensity for hydrophobic interactions. The longer alkyl side chains of OMBF will also mediate stronger hydrophobic interactions compared with HMF.

3.6- Semi-empirical quantum mechanical calculations

The multi-point hydrogen bonded complexes of HMF and OMBF with amino acid residues of BSA were analysed by using PM6-D3H+. The semi-empirical method, despite being computationally inexpensive, has been successfully used to determine interaction energies that rival in accuracy results obtained with DFT [18]. The

optimised geometry of the investigated complexes by using the PM6-D3H+ method is demonstrated in Figure 7. The coordinates of the complexes are reproduced in the supplemental files. Analysis by using the same method ruled out the existence of imaginary frequencies and confirmed that convergence was achieved. The heat of formation, frontier molecular orbitals, and the interaction energies of HMF and OMBF

complexes are represented in Table 2. The interaction energy of OMBF-BSA complex was 1.5 folds higher than that of HMF. This trend was consistent with molecular docking studies. Therefore, OMBF formed a more stable complex with BSA compared with HMF. The energy gaps of both ligands were also within feasible transition levels.

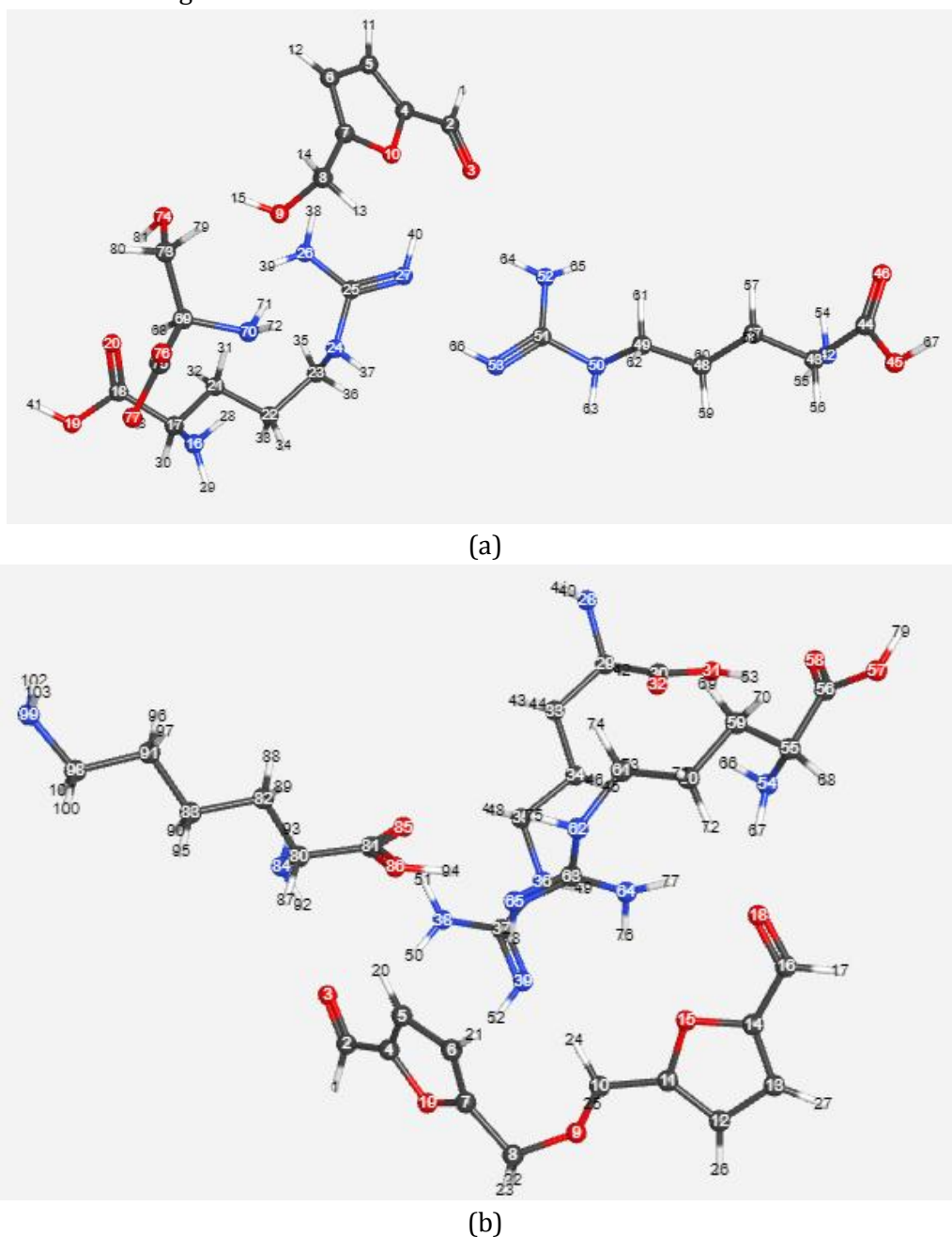


Fig. 7. Optimised structures of (a) HMF and (b) OMBF complex within the PM6-D3H+ approximations

Table 2. Geometrical parameters and interaction energy (ΔE) of HMF and OMBF complexes by using PM6-D3H+

Complex	Heat of formation (kcal/mol)	HOMO (eV)	LUMO (eV)	ΔE (kcal/mol)
HMF-BSA	-405.49	-9.14	-1.39	-51.43
OMBF-BSA	-420.53	-9.16	-1.57	-76.27

4-Conclusion

The binding interactions of HMF and OMBF with BSA were studied by using the UV-visible spectroscopic, molecular docking, and semi-empirical methods. Spectroscopic results showed that OMBF induced more perturbations in the 278 nm electronic absorption band of BSA compared with HMF. Furthermore, the degradant formed a more stable complex with BSA with a binding constant ($\ln K_b$) of 8.99 compared with 5.97 obtained with HMF.

Thermodynamic investigations identified hydrophobic interactions as the major forces driving the interaction of BSA with both OMBF and HMF. Molecular modelling showed that although both ligands occupied the hydrophobic pocket of Site I of BSA, the OMBF binding was characterized by a higher binding energy of 7.2 kcal/mol attributed to the more extensive hydrophobic interactions between the aromatic rings of the ligand and hydrophobic residues of BSA. Semi-empirical calculations also corroborated the observed trend with the interaction energy of OMBF-BSA complex being 1.5 folds greater than that of HMF. Therefore, this study confirmed an increased avidity and stability in the complexation of albumin with OMBF compared with HMF. The increased affinity of OMBF for albumin might increase its tissue distribution making it more prone to bioaccumulation. A stricter limits control of OMBF in heat-processed foods and parenteral preparations is recommended.

Acknowledgments

The authors acknowledge the assistance of the technical staff of the Multidisciplinary laboratory of the University.

References

- [1]F.J. Morales, Hydroxymethylfurfural (HMF) and related compounds, in: R. Stadler, D.R. Lineback (Eds.), *Process-Induced Food Toxicants: Occurrence, Formation, Mitigation, and Health Risks*, John Wiley and Sons, Inc., New Jersey, (2009) 135–174.
- [2]K. Abraham, R. Gürtler, K. Berg, G. Heinemeyer, A. Lampen, K.E. Appel, Toxicology and risk assessment of 5-Hydroxymethylfurfural in food, *Mol. Nutr. Food Res.*, 55 (2011) 667–678.
<https://doi.org/10.1002/mnfr.201000564>.
- [3]N. Lin, T. Liu, L. Lin, S. Lin, Q. Zang, J. He, Z. Abliz, C. Li, A. Wang, H. Jin, Comparison of in vivo immunomodulatory effects of 5-hydroxymethylfurfural and 5, 5'-oxydimethylenebis (2-furfural), *Regul. Toxicol. Pharmacol.*, 81 (2016) 500–511.
<https://doi.org/https://doi.org/10.1016/j.yrtph.2016.10.008>.
- [4]M.R. Farag, M. Alagawany, M. Bin-Jumah, S.I. Othman, A.F. Khafaga, H.M. Shaheen, D. Samak, A.M. Shehata, A.A. Allam, M.E. Abd El-Hack, The toxicological aspects of the heat-borne toxicant 5-hydroxymethylfurfural in animals: A review, *Molecules*, 25 (2020) 1–13.
<https://doi.org/10.3390/molecules25081941>.

- [5] U.M. Shapla, M. Solayman, N. Alam, M.I. Khalil, S.H. Gan, 5-Hydroxymethylfurfural (HMF) levels in honey and other food products: effects on bees and human health, *Chem. Cent. J.*, 12 (2018) 35.
<https://doi.org/10.1186/s13065-018-0408-3>.
- [6] I. Florin, L. Rutberg, M. Curvall, C.R. Enzell, Screening of tobacco smoke constituents for mutagenicity using the Ames' test, *Toxicology*, 15 (1980) 219–232.
- [7] Y.C. Lee, M. Shlyankevich, H.-K. Jeong, J.S. Douglas, Y.J. Surh, Bioactivation of 5-hydroxymethyl-2-furaldehyde to an electrophilic and mutagenic allylic sulfuric acid ester, *Biochem. Biophys. Res. Commun.*, 209 (1995) 996–1002.
- [8] H. Glatt, H. Schneider, Y. Liu, V79-hCYP2E1-hSULT1A1, a cell line for the sensitive detection of genotoxic effects induced by carbohydrate pyrolysis products and other food-borne chemicals, *Mutat. Res. Toxicol. Environ. Mutagen.*, 580 (2005) 41–52.
- [9] A.H. Høie, C. Svendsen, G. Brunborg, H. Glatt, J. Alexander, W. Meinel, T. Husøy, Genotoxicity of three food processing contaminants in transgenic mice expressing human sulfotransferases 1A1 and 1A2 as assessed by the in vivo alkaline single cell gel electrophoresis assay, *Environ. Mol. Mutagen.*, 56 (2015) 709–714.
<https://doi.org/10.1002/em.21963>.
- [10] L.J.K. Durling, L. Busk, B.E. Hellman, Evaluation of the DNA damaging effect of the heat-induced food toxicant 5-hydroxymethylfurfural (HMF) in various cell lines with different activities of sulfotransferases, *Food Chem. Toxicol.*, 47 (2009) 880–884.
- [11] M. Guo, L. He, X.W. Lu, Binding mechanism of traditional Chinese medicine active component 5-hydroxymethyl-furfural and HSA or BSA, *Yao Xue Xue Bao= Acta Pharm. Sin.*, 47 (2012) 385–392.
- [12] B. Chen, H. Luo, W. Chen, Q. Huang, K. Zheng, D. Xu, Pharmacokinetics, tissue distribution and Human serum albumin binding properties of Delicaflavone, a novel anti-tumor candidate, *Front. Pharmacol.*, 12 (2021) 1–12.
<https://doi.org/10.3389/fphar.2021.761884>.
- [13] O.E. Thomas, O.A. Adegoke, Toxicity of food colours and additives: A review, *African J. Pharm. Pharmacol.*, 9 (2015) 900–914.
<https://doi.org/10.5897/AJPP2015.4385>.
- [14] G. Arribas-Lorenzo, F.J. Morales, Estimation of dietary intake of 5-hydroxymethylfurfural and related substances from coffee to Spanish population, *Food Chem. Toxicol.*, 48 (2010) 644–649.
<https://doi.org/10.1016/j.fct.2009.11.046>.
- [15] B.F.M. Kuster, 5-Hydroxymethylfurfural (HMF): a review focussing on its manufacture, *Starch-Stärke*, 42 (1990) 314–321.
- [16] C. Larousse, L. Rigal, A. Gaset, Synthesis of 5, 5'-Oxydimethylenebis (2-furfural) by Thermal dehydration of 5-Hydroxymethyl-2-furfural in the presence of Dimethylsulfoxide, *J. Chem. Technol. Biotechnol.*, 53 (1992) 111–116.
- [17] C.E. Duru, I.A. Duru, A.E. Adegboyega, In silico identification of compounds from *Nigella sativa* seed oil as potential inhibitors of SARS-CoV-2 targets, *Bull. Natl. Res. Cent.*, 45:57 (2021).
<https://doi.org/10.1186/s42269-021-00517-x>.
- [18] J.C. Kromann, A.S. Christensen, C. Steinmann, M. Korth, J.H. Jensen, A third-generation dispersion and third-generation hydrogen bonding corrected PM6 method: PM6-D3H+, *PeerJ*, 2 (2014) e449
<https://doi.org/10.7717/peerj.449>.
- [19] M. Waller, S. Grimme, Weak intermolecular interactions: A supermolecular approach, in: L. Leszczynski (Ed.), *Handbook of Computational Chemistry*, Springer Science+Business Media, Berlin, (2012) 444–466.

https://doi.org/10.1007/978-94-007-0711-5_12,

- [20] A. Hashim, V. Poulouse, T. Thiemann, One pot o-alkylation/Wittig olefination of hydroxybenzaldehydes in DMSO, *Chem. Proc.*, (2021) 99. <https://doi.org/10.3390/ecsoc-24-08288>
- [21] M. Kazemia, Z. Noori, H. Kohzadi, M. Sayadia, A. Kazemia, A mild and efficient procedure for the synthesis of ethers from various alkyl halides, *Q. J. Iran. Chem. Commun.*, 1 (2013) 43–50.
- [22] A.L. Koritzke, K.M. Frandsen, M.G. Christianson, J.C. Davis, A.C. Doner, A. Larsson, J. Breda-Nixon, B. Rotavera, Fragmentation mechanisms from electron-impact of complex cyclic ethers formed in combustion, *Int. J. Mass Spectrom.*, 454 (2020) e116342.
- [23] O. Herbinet, S. Bax, P.-A. Glaude, V. Carré, F. Battin-Leclerc, Mass spectra of cyclic ethers formed in the low-temperature oxidation of a series of n-alkanes, *Fuel*, 90 (2011) 528–535.
- [24] S.D. Stojanović, J.M. Nićiforović, S.M. Živanović, J. V Odović, R.M. Jelić, Spectroscopic studies on the drug – drug interaction: the influence of fluoroquinolones on the affinity of tigecycline to human serum albumin and identification of the binding site, *Monatshefte Für Chemie - Chem. Mon.*, 151 (2020) 999–1007.
<https://doi.org/10.1007/s00706-020-02627-0>.
- [25] N. Shahabadi, S.M. Fili, Molecular modeling and multispectroscopic studies of the interaction of mesalamine with bovine serum albumin, *Spectrochim. Acta - Part A Mol. Biomol. Spectrosc.*, 118 (2014) 422–429.
<https://doi.org/10.1016/j.saa.2013.08.110>.
- [26] M. Al Bratty, Spectroscopic and molecular docking studies for characterizing binding mechanism and conformational changes of human serum albumin upon interaction with Telmisartan, *Saudi Pharm. J.*, 28 (2020) 729–736.
<https://doi.org/10.1016/j.jsps.2020.04.015>.
- [27] N. Shahabadi, S. Zendehecheshm, Evaluation of ct-DNA and HSA binding propensity of antibacterial drug chloroxine: Multi-spectroscopic analysis, atomic force microscopy and docking simulation, *Spectrochim. Acta Part A Mol. Biomol. Spectrosc.*, 230 (2020) 118042.
<https://doi.org/10.1016/j.saa.2020.118042>.
- [28] S.M. Jankovic, S.D. Stojanovic, Interaction between tigecycline and human serum albumin in aqueous solution, *Monatshefte Fur Chemie.*, 146 (2015) 399–409.
<https://doi.org/10.1007/s00706-014-1330-6>.
- [29] M. Khoder, H. Abdelkader, A. ElShaer, A. Karam, M. Najlah, R.G. Alany, Efficient approach to enhance drug solubility by particle engineering of bovine serum albumin, *Int. J. Pharm.*, 515 (2016) 740–748.
- [30] M. Schauerl, M. Podewitz, B.J. Waldner, K.R. Liedl, Enthalpic and entropic contributions to hydrophobicity, *J. Chem. Theory Comput.*, (2016) 4600-4610
<https://doi.org/10.1021/acs.jctc.6b00422>.
- [31] S. Mukherjee, L.V. Schafer, Spatially resolved hydration thermodynamics in biomolecular systems, *J Phys Chem B*, 126 (2022) 3619–3631.
<https://doi.org/10.1021/acs.jpcc.2c01088>
- [32] R.N. El Gammal, H. Elmansi, A.A. El Emam, F. Belal, M.E. Hammouda, Exploring the molecular interaction of mebendazole with bovine serum albumin using multi-spectroscopic approaches and molecular docking, *Sci Rep.*, 12 (2022) 11582.
<https://doi.org/doi:10.1038/s41598-022-15696-4>.
- [33] Z. Zhou, X. Hu, X. Hong, J. Zheng, X. Liu, D. Gong, G. Zhang, Interaction characterization of 5-hydroxymethyl-2-furaldehyde with human serum albumin: binding characteristics, conformational change and mechanism, *J. Mol. Liq.*, (2019) 111835.
<https://doi.org/10.1016/j.molliq.2019.111835>.

- [34] C. Pommié, S. Levadoux, R. Sabatier, G. Lefranc, M. Lefranc, IMGT standardized criteria for statistical analysis of immunoglobulin V-REGION amino acid properties, *J. Mol. Recognit.*, 17 (2004) 17–32. <https://doi.org/10.1002/jmr.647>.

HOW TO CITE THIS ARTICLE

Olusegun Emmanuel Thomas*, Rashidat Temitope Oduwale. Spectroscopic, Molecular Docking and Semi-Empirical Studies of the Albumin Binding Activities of 5-Hydroxymethylfurfural and its Synthesized Derivative, Di (5-Furfural) Ether, *Prog. Chem. Biochem. Res.*, 5(3) (2022) 239-253.

DOI: 10.22034/pcbr.2022.349903.1226

URL: http://www.pcbiochemres.com/article_158123.html

